Supplementary Materials

Highly Shape-Morphable Origami Electromagnetic Waveguides

Nikhil Ashok,[1] Sangwoo Suk,[1] Sven G. Bilén,[2] and Xin Ning[1] *

[1]Department of Aerospace Engineering, University of Illinois Urbana-Champaign

[2]School of Engineering Design and Innovation, Department of Electrical Engineering, and Department of Aerospace Engineering, The Pennsylvania State University

*Corresponding author: xning@illinois.edu

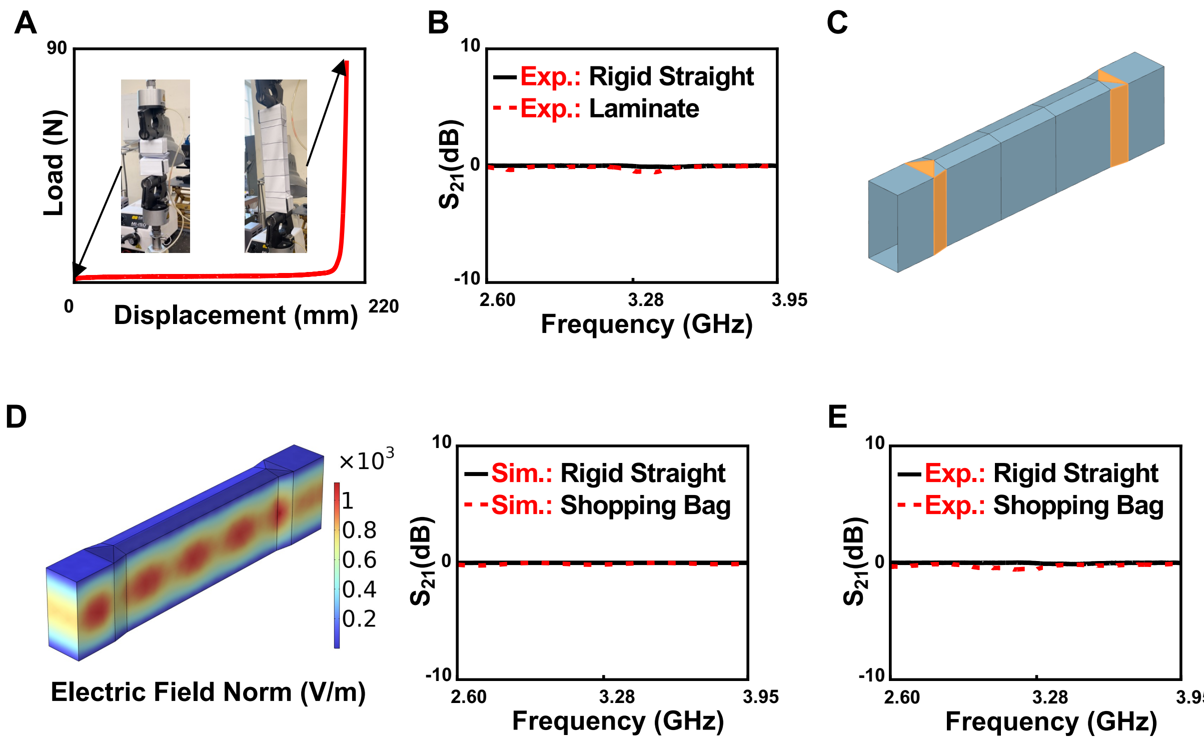

Figure S1. Mechanical testing and microwave transmission performance of shopping-bag waveguides. (A) Load vs. displacement curve obtained by performing a uniaxial tension test on a concave shopping-bag model. **(B)** Experimental S_{21} vs. frequency plots, presenting a performance comparison between the WR-284 straight waveguide and the fabricated laminate waveguide. **(C)** CAD model of a shopping-bag waveguide with convex narrow walls. **(D)** Simulation results of the electric field distribution at the central frequency (left) and the S_{21} vs. frequency plots (right), providing a comparative analysis between the baseline WR-284 straight waveguide and the shopping-bag waveguide (convex design). **(E)** Experimental S_{21} vs. frequency plots, presenting a performance comparison between the WR-284 straight waveguide and the fabricated shopping-bag waveguide (convex design).

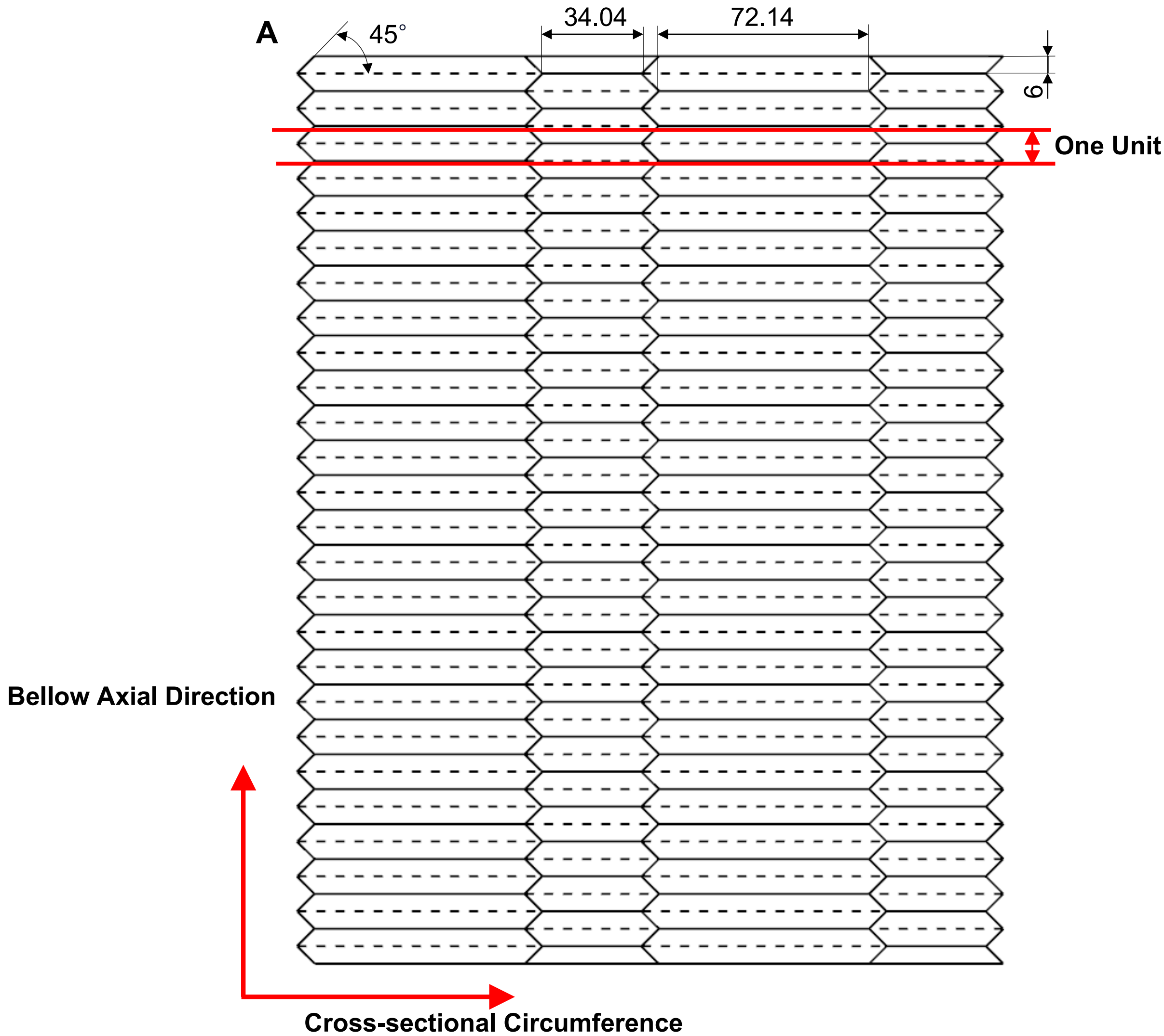

Figure S2. Origami folding pattern adopted to fabricate the straight bellows waveguide. All dimensions are in mm.

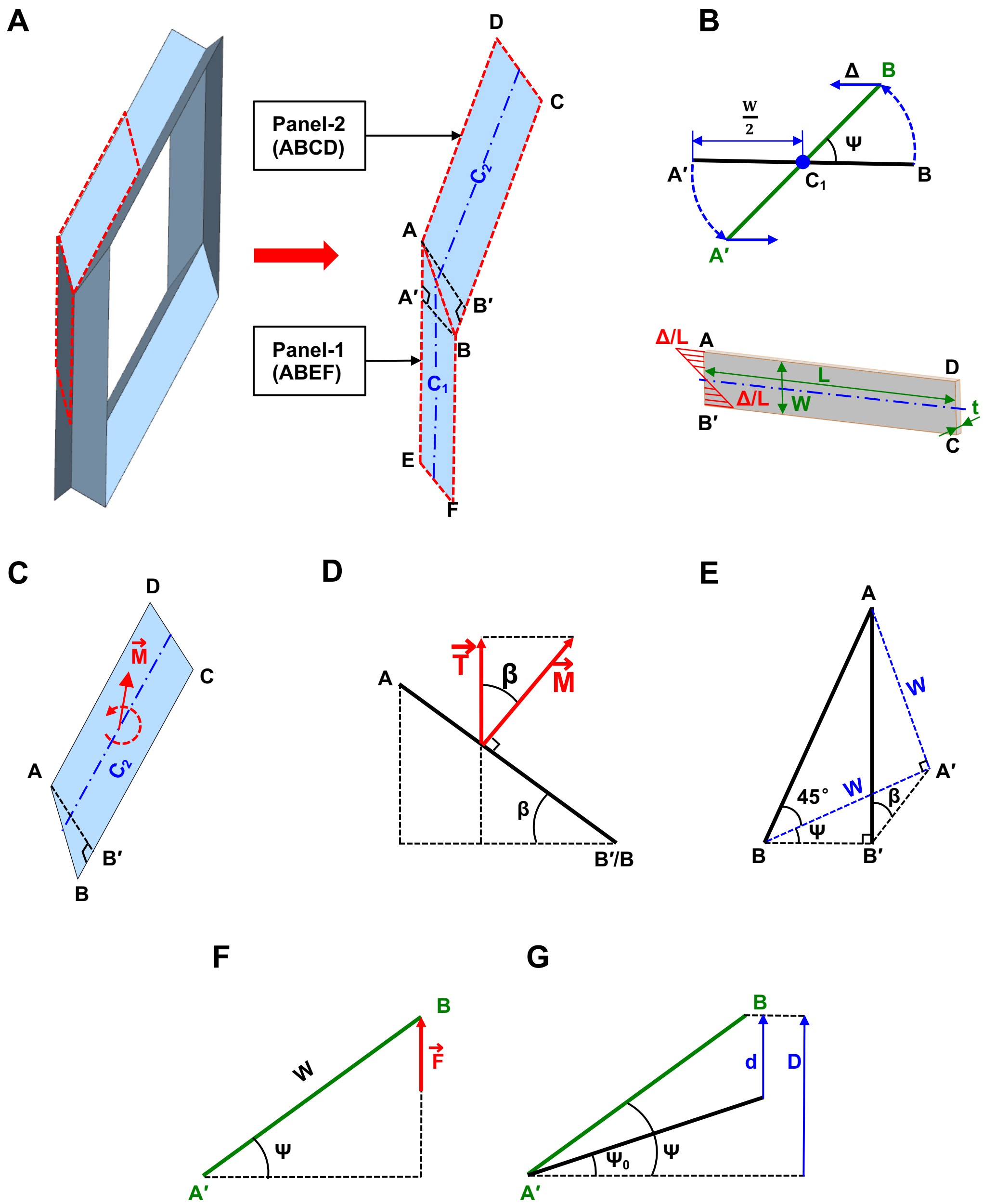

Figure S3. Mechanics associated with the straight bellows model. (A) Unit bellows model with one-eight highlighted portion under study. **(B)** Rotation of the line A'B about C_1 axis (top) creates in-plane bending in panel-2 (bottom). **(C)** Bending moment acting on panel-2. **(D)** The component of moment T creates twisting in panel-1. **(E)** Diagram that relates angle β and the deployment angle Ψ. **(F)** Top view of panel-1 indicating the application of the external force F. **(G)** Diagram depicting the extended displacement (d) and opening length (D).

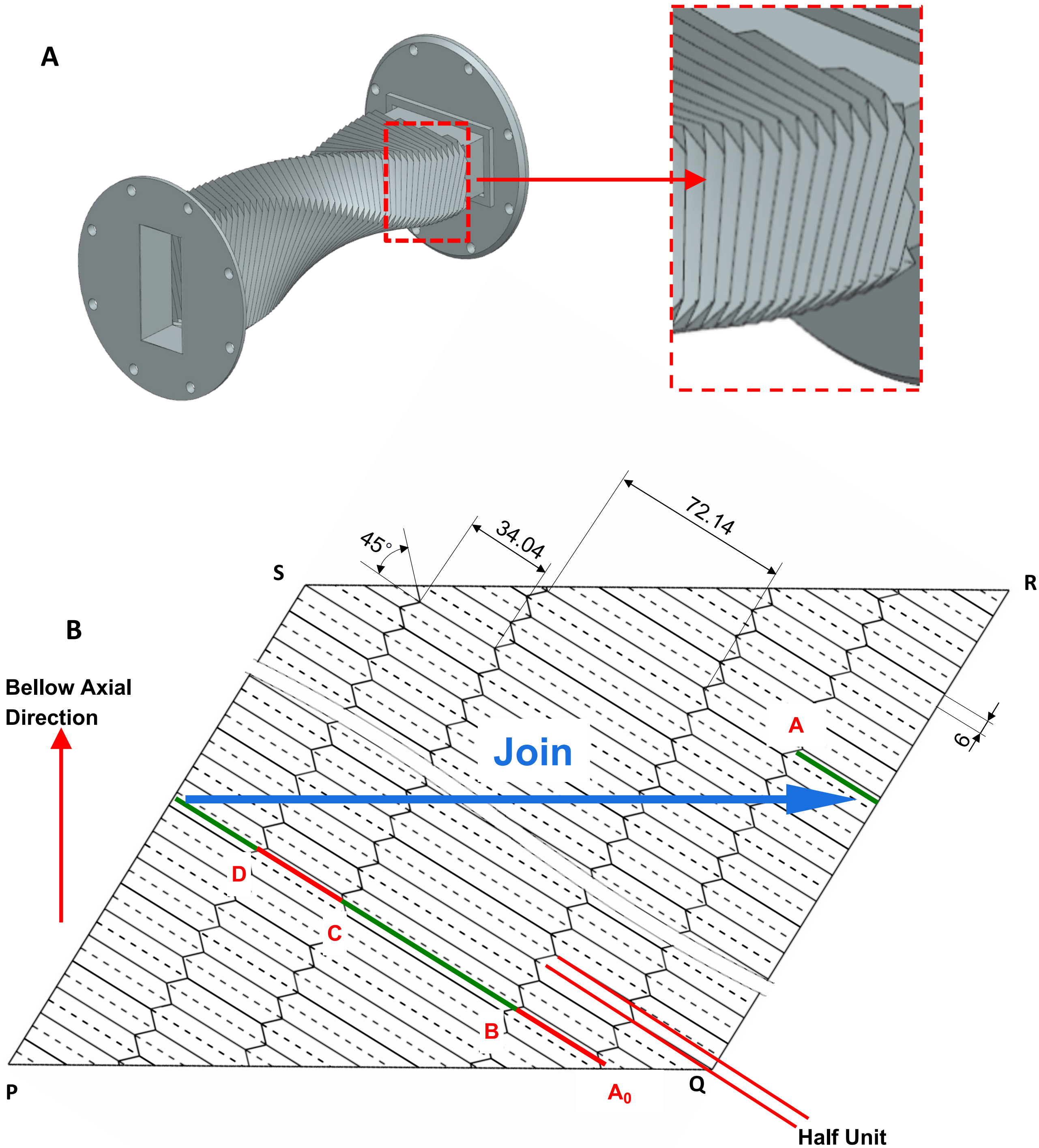

Figure S4. Twist bellows geometry, folding pattern, and its dimensions. (A) CAD model and a zoomed-in view of the constituent units. **(B)** Origami pattern adopted to fabricate the twist bellows waveguide. All dimensions are in mm.

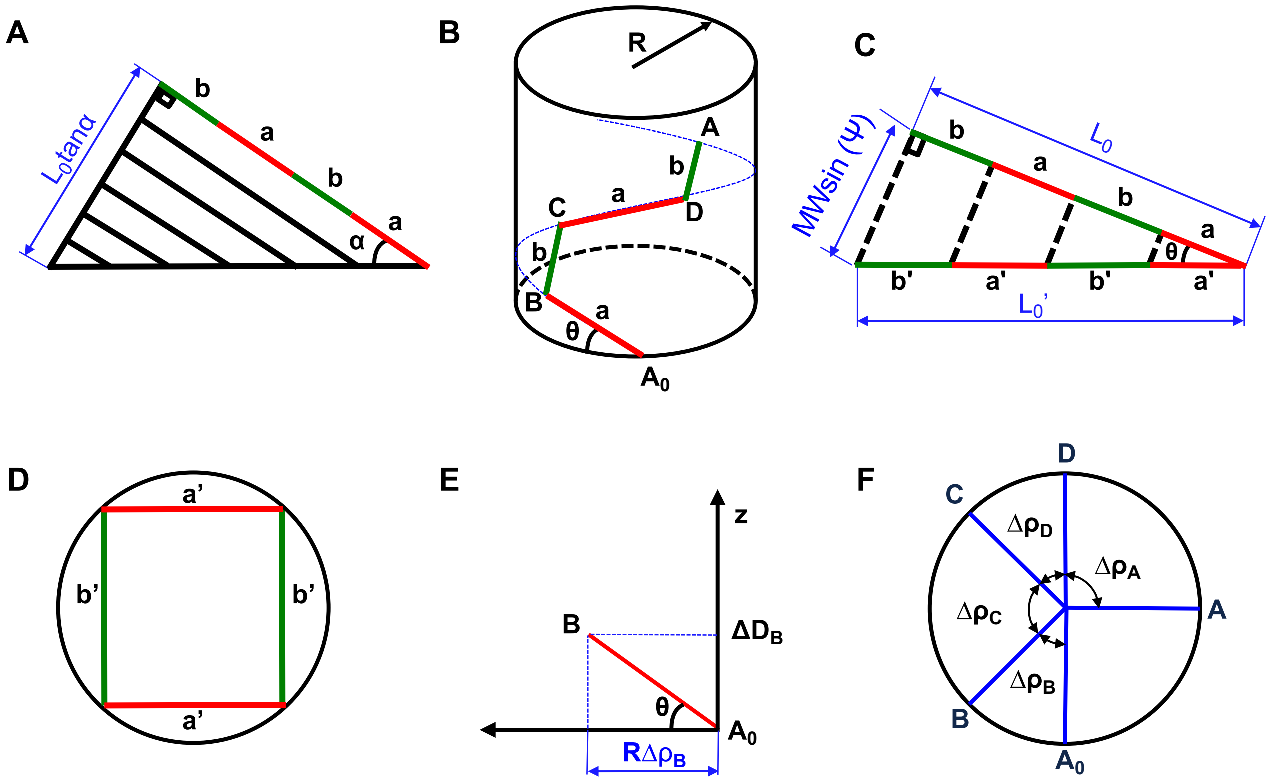

Figure S5. Kinematics analyses of a twistable bellows EM waveguide. (A) Repeated segment of the 2D crease pattern used in the twist bellows model, highlighting fixed-length sections. a and b denote the fixed lengths of the short and long creases. **(B)** A continuous crease circumscribed by a cylinder of radius R when the twist bellow deploys at angle θ with point A_0 fixed as a reference. The endpoints of each crease follow a helical path during deployment. **(C)** Projection of the fixed lengths onto the horizontal plane after deployment. **(D)** Top view of the cylinder with the projected lines in (C). **(E)** Expansion of the cylinder into a flat plane highlighting the crease A_0B. **(F)** Top view of the cylinder with the deployed creases, showing the rotation angle ρ about the previous point.

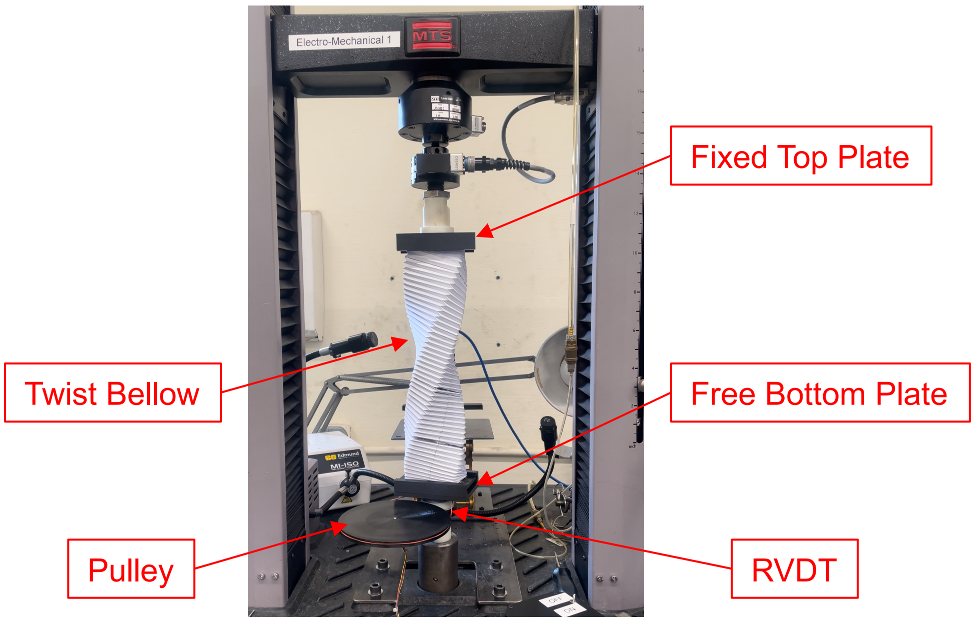

Figure S6. The experimental set-up for the deployment test on the twist bellow model.

Table S1. The difference in experimental mean transmission loss between a configuration and the baseline waveguide and the standard deviation between 10 experiments

Experimental Results		
Configuration	**Mean($\|S_{21}\|_{config.}$) − Mean($\|S_{21}\|_{baseline}$) (dB)**	**Standard Deviation**
Laminate Waveguide	0.13	-
Shopping Bag (Concave Design)	0.14	0.02
Shopping Bag (Convex Design)	0.25	0.02
Straight Bellow ($N = 26$, $W = 6$ mm)	0.85	0.04
Straight Bellow Partially Deployed	0.80	0.04
Straight Bellow Fully Compressed	1.17	0.07
E-Bend Bellow	0.84	0.04
H-Bend Bellow	0.94	0.04
Twist Bellow	0.70	0.03

Table S2. The difference in simulation mean transmission loss between a configuration and the baseline waveguide

Simulation Results	
Configuration	**Mean($\|S_{21}\|_{config.}$) − Mean($\|S_{21}\|_{baseline}$) (dB)**
Shopping Bag (Concave Design)	0.04
Shopping Bag (Convex Design)	0.09
Straight Bellow ($N = 26$, $w = 6$ mm)	0.02
Straight Bellow Partially Deployed	0.02
Straight Bellow Fully Compressed	0.01
Straight Bellow ($N = 26$, $w = 9$ mm)	0.04
Straight Bellow ($N = 26$, $w = 12$ mm)	0.08
Straight Bellow ($N = 21$, $w = 6$ mm)	0.02
Straight Bellow ($N = 26$, $w = 6$ mm)	0.02
Straight Bellow ($N = 31$, $w = 6$ mm)	0.02
Twist Bellow	0.02
E-Bend Bellow	-0.09
H-Bend Bellow	0.02

Supplementary Text 1: Mechanics of Straight Bellows Waveguide Deployment

Focusing on a single unit of the bellows as shown on the left in Figure S3A, we replicate this unit to form the complete structure. Taking advantage of the bellows' symmetry, we focus our analysis on a section of the unit, illustrated on the right of Figure S3A composed of panel 1 (ABEF) and panel 2 (ABCD). Here, we assume that panel 1 acts as a rigid panel and panel 2 as an elastic panel. Panel 1 can rotate about the center line C_1 as the bellows model deploys. This is depicted through the motion of the normal line A′B of length W shown in the top of Figure S3B. As the bellows deploys by a distance Δ, line A′B rotates about C_1 by an angle Ψ referred to as the deployment angle. Different values of Ψ indicate different stages of deployment with Ψ = 0° and Ψ = 90° representing the fully compressed and fully deployed stages respectively of the bellows model. $\Psi = \Psi_0$ represents the natural angle which is the zero strain angle when no external force is applied to the model.

As panel 2 is elastic, the rotation of line A′B generates strains in panel 2. Here we assume that the hill AD and valley B′/BC always remain horizontal. Hence the rotation of panel 1 creates in-plane bending of panel 2. This results in tension on the hill AD by Δ and compression on the valley BC by the same distance Δ as depicted in the bottom of Figure S3B. The equation for Δ can be calculated through trigonometric relations and is given by:

$$\Delta = \frac{W(1 - \cos\Psi)}{2} \quad \text{if } \Psi_0 = 0 \tag{1}$$

A more general description of the distance Δ is given by:

$$\Delta = \frac{W(\cos\Psi_0 - \cos\Psi)}{2} \quad \text{if } \Psi_0 \neq 0 \tag{2}$$

Assuming that the points B and B′ on panel 2 have the same strains, the strains at points A and B can be calculated as:

$$\varepsilon_A = +\frac{\Delta}{L};\ \varepsilon_B = -\frac{\Delta}{L} \tag{3}$$

Here, L represents the length of AD or B′C as shown in the bottom of Figure S3B. The bending moment M generated on panel 2 as depicted in Figure S3C is given by:

$$M = KEI \tag{4}$$

K represents the curvature of the beam AB′CD, E the elastic modulus, and I the area moment of inertia. The equation for K is given by:

$$K = \frac{\varepsilon_A}{(\frac{W}{2})} = \frac{\Delta}{L}\frac{1}{(\frac{W}{2})} = \frac{2\Delta}{WL} \tag{5}$$

For a panel of width W and thickness t, the equation for the moment of inertia I is given by:

$$\mathrm{I} = \frac{1}{12}tW^3 \tag{6}$$

By substituting Equation (*5*) and (*6*) into Equation (*4*) we get:

$$M = KEI = \frac{2\Delta}{WL}E\frac{1}{12}tW^3 = \frac{1}{6}Et\frac{\Delta}{L}W^2 \tag{7}$$

The moment acts normal to panel 2. Panel 2 is inclined at an angle β to the horizontal plane as depicted in Figure S3D. The vertical component of M is given by:

$$T = M\cos\beta \tag{8}$$

Here, T is the twisting moment applied on panel 1. Next, based on Figure S3E, a relation between angle β and the deployment angle Ψ is derived as detailed below:

$$\begin{gathered} \mathrm{AA'} = W,\ \ \mathrm{A'B} = W \\ \mathrm{A'B'} = W\sin\Psi \Rightarrow \mathrm{AB'} = \sqrt{W^2 + W^2\sin^2\Psi} = W\sqrt{1+\sin^2\Psi} \\ \therefore \cos\beta = \frac{\sin\Psi}{\sqrt{1+\sin^2\Psi}} \end{gathered} \tag{9}$$

Combining Equations (*7*), (*8*), and (*9*):

$$T{=}M\cos\beta = \frac{1}{6}Et\frac{\Delta}{L}W^2\frac{\sin\Psi}{\sqrt{1+\sin^2\Psi}} \tag{10}$$

Substituting the equation for Δ given in Equation (*2*) into Equation (*10*):

$$T{=}\ \frac{1}{12}Et\frac{1}{L}W^3(\cos\Psi_0 - \cos\Psi)\frac{\sin\Psi}{\sqrt{1+\sin^2\Psi}} \tag{11}$$

The twisting moment T is balanced by the moment created by the actuation force F as illustrated in Figure S3F. Hence, the equation for T is given by:

$$T{=}FW\cos\Psi \tag{12}$$

By equating Equations (*11*) and (*12*)(*12*) we obtain the following result:

$$F{=}\ \frac{1}{12}Et\frac{1}{L}W^2(\cos\Psi_0 - \cos\Psi)\frac{\sin\Psi}{\sqrt{1+\sin^2\Psi}}\ \frac{1}{\cos\Psi} \tag{13}$$

The non-dimensionalized form of the force F_n is given by:

$$F_n{=}\frac{F}{\frac{1}{12}Et\frac{1}{L}W^2} = (\cos\Psi_0 - \cos\Psi)\frac{\sin\Psi}{\sqrt{1+\sin^2\Psi}}\ \frac{1}{\cos\Psi} \tag{14}$$

Also, the extended displacement d depicted in Figure S3G can be calculated using trigonometric relations. d and its non-dimensionalized form d_n is given by:

$$d{=}W(\sin\Psi\text{-}\sin\Psi_0)$$

$$d_n{=}\ \frac{d}{W} = (\sin\Psi\text{-}\sin\Psi_0) \tag{15}$$

Similarly, the current opening length D shown in Figure S3G and its normalized form D_n is given by:

$$D = W \sin \Psi \Rightarrow \frac{D}{W} = \sin \Psi = D_n \tag{16}$$

Supplementary Text 2: Deployment Motion Analyses of Twist Bellow Waveguide

Consider the 2D crease pattern shown in Figure S5A, where a and b denote the fixed lengths of the short and long creases, respectively, and the total diagonal length L_0 equals $2(a + b)$, as illustrated. Let α represent the cut angle, as shown in Figure S5A. If W represents the width of a facet of a half unit, then the equation for the number of half units, M is given by:

$$M = L_0 \frac{\tan \alpha}{W} \tag{17}$$

Folding the crease pattern generates the twist bellow, which rotates as it deploys. The height at which a 90° rotation occurs depends on the values of α and M and should match the height of the rigid twist waveguide. The steps below detail the method used to determine the relationship between the rotation angle and the deployment length for a given α.

This relation is determined based on two assumptions. The first assumes that during all stages of deployment, the conner points of a crease line (i.e., A/A_0, B, C, and D) lie on a cylinder. Figure S5B illustrates this, showing a continuous crease of four segments of lengths a and b in its deployed configuration. All points at the conners lie on a cylinder of radius R. The second assumption is that all the crease conner points follow a helical path during deployment, as depicted in the deployed configuration in Figure S5B. As the angle θ increases, the pitch of the helix also increases.

Figure S5C shows the crease expanded to a 2D plane at a generic helix angle θ. The lengths a' and b' represent the projected length on the horizontal axis with the total length being L_0'. The line L_0' forms a rectangle on the bottom when folded as depicted in Figure S5D. Similar to the straight bellow, Ψ represents the deployment angle and the deployment distance of a half-unit is $W \sin \Psi$. Hence, the deployment distance for M half-units would be $MW \sin \Psi$. Using Equation (17), this distance can be expressed as:

$$MW \sin \Psi = L_0 \tan \alpha \, \sin \Psi \tag{18}$$

The distance L_0' can be calculated as:

$$L_0' = L_0 \sqrt{1 + (\tan \alpha \, \sin \Psi)^2} \tag{19}$$

The cosine and tangent values of angle θ can be calculated as:

$$\cos\theta = \frac{1}{\sqrt{1+(\tan\alpha\ \sin\Psi)^2}} \tag{20}$$

$$\tan\theta = \tan\alpha \sin\Psi \tag{21}$$

Let λ represent the ratio b/a, the following relations can be inferred from Figure S5C:

$$\frac{b}{a} = \frac{b'}{a'} = \lambda;\ \text{where } a' = \frac{a}{\cos\theta}\ ,\ b' = \frac{b}{\cos\theta} \tag{22}$$

$$2(a'+b') = L_0' \tag{23}$$

$$a'^2 + b'^2 = 4R^2 \tag{24}$$

Note that since the lengths a' and b' depicted in Equation (22) changes with angle θ, results in the radius R calculated using Equation (24) also change as the twist bellow deploys. Combining Equations (22), (23) and (24) we get:

$$\left(1+\lambda^2\right)\frac{a^2}{\cos^2\theta} = 4R^2 \Rightarrow \frac{a}{R} = \frac{2\cos\theta}{\sqrt{1+\lambda^2}} \tag{25}$$

$$\text{Also, } \frac{b}{R} = \frac{\lambda a}{R} \tag{26}$$

Equations (25) and (26) relate the cylinder's radius with the segments' fixed length. Next, the cylinder expands into a flat plane with one segment A_0B highlighted, as shown in Figure S5E. In this configuration, ρ represents the angular position around the z-axis, as indicated in Figure S5F, referred to as the rotation angle. From Figure S5E, the height ΔD_B and the coordinates of point B in the cylindrical coordinate system are given by:

$$\Delta D_B = R\Delta\rho_B \tan\theta \tag{27}$$

$$B = (R,\ \Delta\rho_B,\ R\Delta\rho_B \tan\theta) \tag{28}$$

In the Cartesian coordinate system, the coordinates of the points A_0 and B are given:

$$A_0=(R,0,0) \tag{29}$$

$$B= (R\cos\Delta\rho_B, R\sin\Delta\rho_B, R\Delta\rho_B\tan\theta) \tag{30}$$

Since the stretching of the panels are small, the distance A_0-B is can be considered to be a constant a, calculated using Equations (28) and (29) and is given by:

$$\begin{gathered} R^2\left(\cos\Delta\rho_B\text{-}1\right)^2+R^2\sin^2\Delta\rho_B+R^2\Delta\rho_B^2\tan^2\theta=a^2 \\ \Rightarrow\left(\cos\Delta\rho_B\text{-}1\right)^2+\sin^2\Delta\rho_B+\Delta\rho_B^2\tan^2\theta=\left(\frac{a}{R}\right)^2 \\ \Rightarrow 2\text{-}2\cos\Delta\rho_B+\Delta\rho_B^2\tan^2\theta=\left(\frac{a}{R}\right)^2 \end{gathered} \tag{31}$$

Substituting $\tan\theta$ in Equation (*21*) and $\frac{a}{R}$ in Equation (*25*), and $\cos\theta$ in Equation (*20*) in Equation (*31*) yields:

$$2\text{-}2\cos\Delta\rho_B+\Delta\rho_B^2(\tan\alpha\ \sin\Psi)^2=\frac{4}{(1+\lambda^2)(1+(\tan\alpha\ \sin\Psi)^2)} \tag{32}$$

In Equation (32), angle α is the crease pattern cut angle and Ψ represents the deployment angle. For a given value of α, the relative rotation between B and A_0, $\Delta\rho_B$, can be numerically calculated by solving Equation (32). Repeating the process can find other relative rotations $\Delta\rho_C$, $\Delta\rho_D$, and $\Delta\rho_A$, as shown in Figure S5F. The relative angle between A and A_0 changes from zero when the structure is fully folded (i.e., A and A_0 coincide) to a non-zero value ρ after the structure is extended:

$$\rho = 2\pi\text{-}(\Delta\rho_B+\Delta\rho_C+\Delta\rho_D+\Delta\rho_A) \tag{33}$$

We use similar relations in Equation (27) to find the height of point A, D_A, given as:

$$D_A = R(\Delta\rho_B + \Delta\rho_C + \Delta\rho_D + \Delta\rho_A)\tan\theta \tag{34}$$

Rearranging and substituting for $\tan\theta$ from Equation (21) we get:

$$\frac{D_A}{R} = (\Delta\rho_B + \Delta\rho_C + \Delta\rho_D + \Delta\rho_A)\ \tan\alpha\sin\Psi \tag{35}$$

Since the cylinder radius R changes, we normalize it over the fixed length L_0. Hence, we get:

$$\frac{D_A}{L_0} = \frac{D_A/R}{L_0/R} = \frac{D_A/R}{2(a+b)/R} = \frac{D_A/R}{\frac{2a}{R} + \frac{2b}{R}} \tag{36}$$

Substituting Equations (25), (26), and (35) in to Equation (36) we obtain the relationship shown below:

$$\frac{D_A}{L_0} = \frac{\left(\Delta\rho_B + \Delta\rho_C + \Delta\rho_D + \Delta\rho_A\right)\tan\alpha\sin\Psi}{\frac{2(1+\lambda)\cos\theta}{\sqrt{1+\lambda^2}}} \tag{37}$$

Since there are M half units in triangular shape (Figure S5A) involved in this analysis, the height and rotation are normalized per half unit as depicted below:

$$D_n = \frac{D_A}{L_0 M} \tag{38}$$

$$\rho_n = \frac{\rho}{M} \tag{39}$$